Tellus (1980), *32*, 251–260

Particle size distribution and optical properties of Arctic haze

By JOST HEINTZENBERG, *Department of Meteorology,*[1] *University of Stockholm, Arrhenius Laboratory, S-106 91 Stockholm, Sweden*

(Manuscript received October 18; in final form December 5 1979)

ABSTRACT

Simultaneous aerosol measurements with particle counters and a multiwavelength integrating nephelometer have been made at Ny-Ålesund, Svalbard (12° E, 79° N). The measured integral aerosol properties were used in an inversion procedure to derive a consistent model of the particle size distribution of Arctic haze. The obtained size distribution is compared to the global background aerosol size distribution. Both the light scattering coefficients and the total suspended volume of particles were found to be on the level of the global background.

1. Introduction

The Arctic is one of the few areas where only very limited knowledge exists about the regional aerosol. Several reasons can be given for this fact. Judging from the global distribution of aerosol sources and the residence times of the particles due to the combination of all the removal processes in the atmosphere, the Arctic should be a very remote area without a strong aerosol burden. The extremely low turbidities and particle concentrations observed in polar air masses that had been transported rapidly to midlatitudes seemed to support the hypothesis of a very clean Arctic air. Data from Antarctica that were extrapolated to the Arctic superficially tended to support this picture. The first exploratory Arctic aerosol measurements about two decades ago gave rather qualitative results (Fenn et al., 1959; Fenn, 1960). However, they also indicated a nearly particle-free Arctic region. Particle concentrations both in the fine particle range under 0.1 μm radius and in the accumulation range of 0.1 μm to 1 μm radius (see Whitby, 1978, for definitions) were found to be close to or below the detection limits of ca 20 cm^{-3} and 0.02 cm^{-3} in the respective size ranges. After the Arctic winter night during March only about 1/100 of the concentrations found during August were measured.

On the other hand later trace gas measurements on the Greenland ice cap showed occasional high CO concentrations in Northern Greenland, which could be correlated with trajectories from the urbanized Great Lakes and New England areas of the U.S. A strong change in composition of the aerosol of Canada's Northwest Territories between summer and winter was observed by Rahn (1971). The winter aerosol was found much more polluted than during summertime. Flyger et al. (1973) found a mean value of total nuclei concentration of the Greenland ice cap around 300 cm^{-3} in summer, which is 15 times higher than the concentrations reported by Fenn et al. (1959). Subsequent aerosol analysis of Rahn et al. (1977) in Northern Alaska supported his earlier findings and an Arctic air-sampling network was installed to document the area-wide distribution of this "imported" aerosol, its sources and its flow patterns into the Arctic (Rahn, 1978). All these results are quite contradictory to those of earlier investigations and justify further and more detailed studies of the Arctic aerosol.

Our knowledge of the optical properties of the Arctic haze is even more sparse and the results just as inconsistent. While the first *in situ* measurements of the light scattering coefficient of Arctic aerosol

[1] Contribution number 404.

0040-2826/80/030251-10$02.50/0

particles at Point Barrow, Alaska yielded a value of $1.1.10^{-5}$ m^{-1} at 0.55 μm wavelength (Porch et al., 1970), Shaw (1975) reported results of solar extinction measurements at the same location with the aerosol particles having 10 times higher extinction coefficients. Obviously more information on the optical properties of Arctic haze from other locations, based on sensitive and well-calibrated methods, is needed.

In an attempt to gather new and reliable information on both particle size distribution and optical properties of the Arctic aerosol, the author conducted a field experiment near Ny-Ålesund, Svalbard, in April–May 1979. Using several particle counters and a multiwavelength integrating nephelometer, a 19-day continuous record of 12 *in situ* aerosol properties was recorded. In the following sections the experiment is described and the results are evaluated and compared to aerosol measurements from other remote locations.

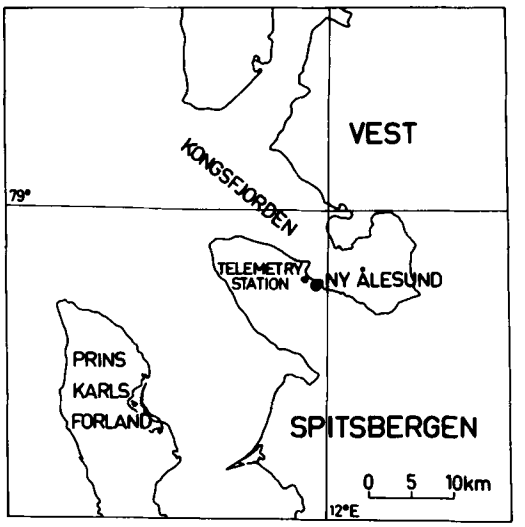

Fig. 1. Map showing measurement location near Ny-Ålesund, Svalbard.

2. Location

When choosing a measuring site for the study of the Arctic aerosol, one faces the usual problems connected with aerosol or trace gas measurements in remote areas. The location should be

(a) representative of a large region
(b) free from local aerosol sources
(c) equipped with sufficient electric power and laboratory space
(d) easily accessible.

There is no such ideal background measuring station and compromises had to be made when choosing Ny-Ålesund, Svalbard, as the measuring site.

The geographical coordinates of Ny-Ålesund are 12° E, 79° N. Thus, it is one of the two northernmost stations of the Arctic air-sampling network allowing the extension of *in situ* aerosol measurements into the deep Arctic. The local emissions are (in their order of importance) the central power and heating plant, ground and air traffic. Because of the absence of significant natural fine particle sources, the local emissions could be identified very clearly. Increases by factors of 10^1–10^3 in the total particle concentration were recorded when local emissions reached the measuring site which was located in an unused telemetry station about 1.5 km away from the settlement. All water and land areas depicted in Fig. 1 were covered with snow and ice throughout the experiment, with the exception of a small open water area west of Kongsfjorden during the last days of the campaign.

3 Instrumentation

All analysis of particle size distribution and light scattering properties of the aerosol were done with *in situ* methods, i.e. through maintaining the airborne state of the particles during the measurement. The instruments, however, had to be located in a heated laboratory. By making use of a 20 x 20 cm former air conditioning channel and a large centrifugal blower (main fan in Fig. 2), the air was rapidly brought from the roof top level into the laboratory. The residence time in the air intake system was under 4 sec. The flow connections between the main stream and the instruments were kept to a minimum length and sharp bends were avoided minimizing by this arrangement the particle losses in the intake. For particles between 0.1 and 5 μm radius no losses were taken into account (Ström, 1972). The loss of Aitken nuclei, however, could not be neglected. It was corrected for by independent measurements with an absolute condensation nuclei counter outside the building, see Section 4.

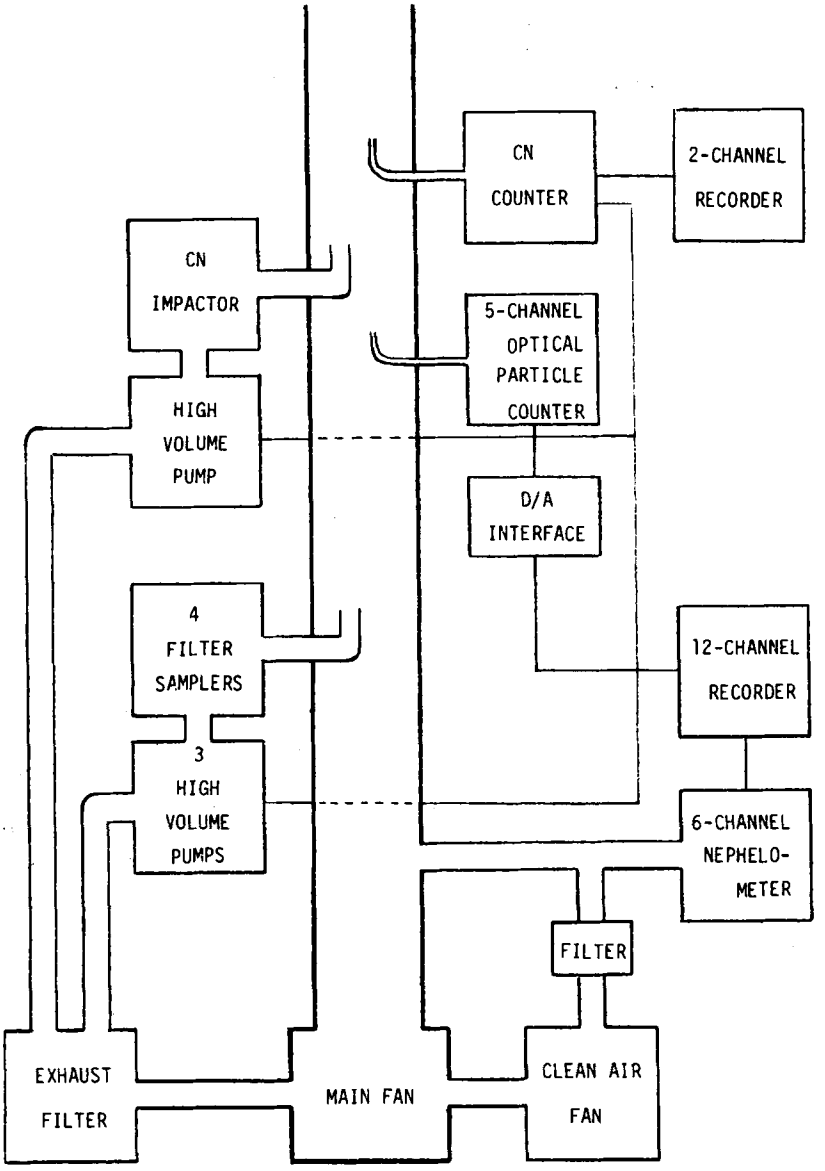

Fig. 2. Schematic air intake and instrument arrangement for the Arctic haze experiment at Ny-Ålesund, Svalbard.

A list of the instruments together with the measured aerosol parameters and the particle size range for each instrument channel are given in Table 1. The technical description of the nephelometer can be found in Charlson et al. (1974). Here is stressed only that the instrument is self-calibrating at both ends of its sensitivity range. An additional absolute calibration with a calibrating gas is performed at regular intervals. An analysis of the systematic errors inherent with nephelometer data has been given by Heintzenberg et al. (1972) and Heintzenberg (1978). The principle of the recording condensation nuclei counter (CNC) is described by Skala (1963) while its size range has been analysed by Haaf et al. (1977). However, through changes in the electronic circuit and improvements in the optical system, the detection limit could be lowered to less

Table 1. *Instrumentation in the Arctic haze study Ny-Ålesund 1979, channel identifications, (ID) measured aerosol parameters and particle size ranges*

Instrument	ID	Measured aerosol parameter		Radius range
3λ	TS1	0.45 μm	Light	All particles
backscatter	TS2	0.55 μm	scattering	dominated by
total scatter	TS3	0.70 μm	integrals	0.1–0.5 μm
integrating	BS1	0.45 μm	in m^{-1}	
nephelometer	BS2	0.55 μm		
	BS3	0.70 μm		
G.E.	CNC	Particle concentration per cm^3		0.002–0.1 μm
condensation nuclei counter				
Royco-225	OPC1	Particle concentration per cm^3		0.20–0.25 μm
optical	OPC2			0.25–0.70 μm
particle	OPC3			0.70–1.50 μm
counter	OPC4			1.50–2.50 μm
	OPC5			>2.50 μm

than 10 cm^{-3}. Because of the above-named intake losses and its basic construction as a relative instrument, it was calibrated with a Scholz-counter (Scholz, 1932) constructed at the Institute for Meteorology, Mainz. A Royco-225 optical particle counter with a 5-channel size discriminator was used to count particles between 0.2 and about 5 μm radius. Liu et al. (1974) have analysed the sensitivity and particle size resolution of the counter. Fig. 2 shows a schematic arrangement of all instruments around the air intake channel. The clean air fan-filter combination is an integral part of the self-calibration circuit of the nephelometer.

With the combination of these three instruments information on physical and optical characteristics of the airborne aerosol was gathered continuously in 12 different channels. The results of the obtained time series are presented in the following section.

4. Primary results

It was the intention of the experiment to determine general characteristics of the Arctic aerosol without the analysis of short term fluctuations and even diurnal variations. Besides this the different instruments required integration times varying between 5 min and 2 h, depending on the level of particle concentrations in the atmosphere. Therefore only hourly averages of the raw data have been evaluated and the results presented here are grand averages over 443 h of operation.

The grand averages as well as positive and negative deviations thereof are summarized in Table 2. The formation of arithmetic grand averages and corresponding relative standard deviations is straightforward and needs no further discussion. When calculating deviations from the averages, it had to be taken into account that the nephelometer channels and particle counter channels are not independent of each other. There is a complicated non-linear relationship between the particle size distribution and the measured spectral light scattering parameters. Therefore the total scattering integral TS2 at 0.55 μm wavelength was chosen as reference parameter when calculating the extremes. The row $\overline{\bar{x}_2 - s_2}$ means that only those readings occurring at times when channel TS2 had values $\bar{x}_2 - s_2$ or below, were averaged. Through this parametric averaging physical meaningful high and low level light scattering spectra and particle counts were derived which could be used in the subsequent data inversion.

Besides the absolute values of the grand averages which will be discussed below, the most remarkable feature of the averaged primary data is their stability with time. Disregarding the channels CNC and OPC 4/5 the standard deviations lie between 30 and 50% compared to one or several orders of magnitude observed in less remote areas. (See for instance Heintzenberg et al. (1979).) The stronger fluctuations in the large particle channels are partly due to the very low particle concentrations recor-

Table 2. *Grand averages ($\bar{x}$) of integrating nephelometer results and particle concentrations for Ny-Ålesund 1979-04-19–1979-05-08, relative standard deviation (s) and average results associated with values of TS2 (scattering coefficient at 0.55 μm) less than TS2 −1 standard deviation and TS2 +1 standard deviation*

	Integrating nephelometer results in 10^{-5} m^{-1}						Particle counter results in cm^{-3} per radius interval					
	TS1	TS2	TS3	BS1	BS2	BS3	CNC	OPC1	OPC2	OPC3	OPC4	OPC5
$\bar{x}$	2.17	1.51	0.955	0.437	0.245	0.195	309	3.8	0.32	0.038	4.1E-3	7.9E-4
s in %	34	33	31	55	28	54	458	33	31	53	98	111
$\bar{x}_2 - s_2$	1.20	0.871	0.562	0.251	0.151	0.204	209	2.4	0.29	0.036	3.8E-3	8.2E-4
$\bar{x}_2 + s_2$	3.31	2.45	1.51	0.525	0.355	0.263	295	6.2	0.42	0.042	5.8E-3	1.0E-3

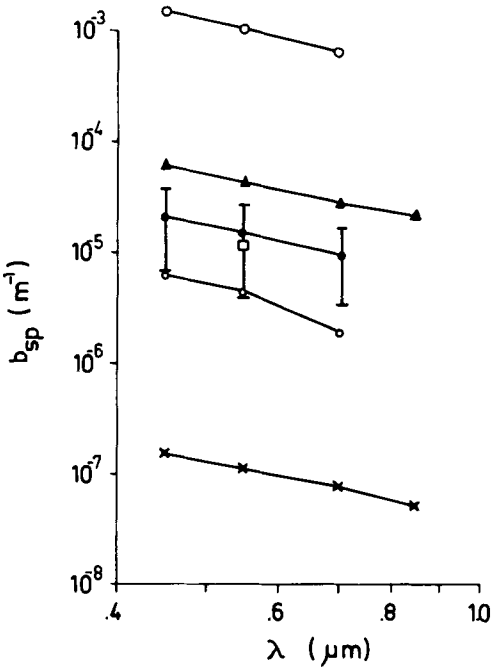

Fig. 3. Spectra of the total light scattering coefficient b_{sp} measured at Ny-Ålesund, Svalbard, according to Table 1 (full circles and error bars). Extreme nephelometer spectra measured at Velen, S. Sweden (open circles), Tsumeb, Namibia (triangles), Barrow, Alaska (square), and Mauna Loa, Hawaii (crosses).

ded in these channels. Another source of fluctuation was snow crystals that were counted occasionally when strong winds caused drifting snow.

The CNC values in Table 2 are corrected for duct losses and background readings with the help of independent measurements with a Scholz counter outside the air intake. The losses were about 50% of the outside concentrations. CN-readings above the most sensitive range of the CN-counter of 300 cm^{-3} were rejected as being locally influenced. However, aged "clouds" of local aerosols drifting over the station probably contributed (besides natural fluctuations) to the high standard deviation in channel CNC.

In Fig. 3 the Svalbard results are compared with spectral nephelometer measurements at other remote locations. The first obvious results of the comparison are:

(a) the light scattering coefficients of the Arctic haze particles lie within the $1–5.10^{-5}$ m^{-1} range which compares well with the results from other remote sea-level locations (Velen, Sweden and Barrow, Alaska);
(b) the Svalbard results agree very well with the only other existing nephelometer measurements in Arctic haze at Barrow, Alaska, and
(c) the Arctic air is not as clean as the high tropospheric background at Mauna Loa but it is not as polluted, either, as a continental background station (Tsumeb, Namibia).

The next step in the evaluation of the data is to combine the information from the light scattering and particle counting instruments to derive a consistent model for the particle size distribution and the optical properties of Arctic haze.

5. The method of data inversion

Inverting atmospheric light scattering data usually means recovering the particle size distribution that caused the observed light scattering. This corresponds to the mathematical problem of finding a solution to the integral equation

$$S_{mj} = \int_0^\infty K_j(x) N^*(x)\, dx \qquad (1)$$

The subscript j refers to the particular measured integral optical properties S_{mj}. $K_j(x)$ is the corresponding kernel of the integral equation and describes the optical effect j of a particle with size coordinate x. An inversion algorithm returns the solution $N^*(x)$ of eq. (1). The number size distribution of the particles $N^*(x)$ is the number of particles with the size x within interval $(x, x + dx)$.

In the case of S_{mj} representing nephelometric measurements the kernels are calculated by applying Mie theory (Mie, 1908) to the actual scattering geometry of the integrating nephelometer. This means the integration of the scattering functions for each particle with size x after weighting with the angular sensitivity function of the actual instrument. Using these integrals (and not the scattering efficients which would assume an ideal integrating nephelometer) one avoids the systematic truncation error that otherwise would spread through the data inversion. However, spherical homogeneous particles of a certain refractive index have to be assumed.

The information of the particle counters is utilized by considering these signals as integral properties S_{mj} in eq. (1). The kernels $K_j(x)$ are zero

outside the size discriminating range of channel j and unity, or a measured counting efficiency, inside the window j of the size discriminator.

The numerical method used here is an improved version of the iterative least square algorithm developed by Heintzenberg (1976) which already has been successfully applied to a number of atmospheric inversion problems. A physically meaningful solution of the integral eq. (1) is constructed as histogram model of the number size distribution of the aerosol particles. Ambiguities in the relation between the size distribution and the measured integral optical properties or particle counts, systematic and statistical errors in the measured quantities have an influence on the goodness of the inversion results. By allowing the values of the measured properties to vary at random within the given range of measuring errors in the course of the inversion, and by repeating the inversion many times over, as an "average solution", an arithmetic mean of the individual solutions to the inversion problem is constructed. One expresses the goodness of a solution in terms of its χ^2

$$\chi^2 = \sum_j \left(\frac{S_{cj} - S_{mj}}{S_{mj}} \right)^2 \qquad (2)$$

S_{cj} being the calculated optical properties or particle counts for the aerosol particle histogram which has been found as solution. It can be shown (H. Schollmayer, private communication) that the $\bar{\chi}^2$ of the "average solution" is as least as good as the average of the χ^2s of the individual solutions that form the average. The statistical character of the total inversion procedure allows the statement of error bars on the derived particle histograms which contain the uncertainties due to measuring errors and the above-named ambiguity. Details about the accuracy of the inversion process alone will be presented in a subsequent paper, Heintzenberg et al. (1980)

In the following part the information of the 12 measured integral aerosol properties will be used in the inversion algorithm to derive a model for the number size distribution of the Arctic haze that exhibits all the physical properties measured on Svalbard.

6. Inversion results

Three averaged sets of light scattering spectra plus integral particle counts were inverted. Besides the grand averages the data associated with TS2 +2 and −1 standard deviation were evaluated. A data set associated with TS2 − 2 standard deviations was not used because there were only two cases available for the calculation of averages.

The inverted number size distributions are collected in Fig. 4. Only the solution for the grand average data set is drawn. The extreme variations in the different histogram columns resulting from the inversion of the other two data sets are contained in the error bars marked at the center of each column. Arrows on certain error bars mean that solutions to the data inversion occur that do not contain any particles in the fine particle columns. To prevent any misinterpretation this effect needs some further explanation. Below about 0.1μm radius the sensitivity of the nephelometer signals to changes in particle concentration decreases with the sixth power of the particle size. Basically, many very small particles can cause the

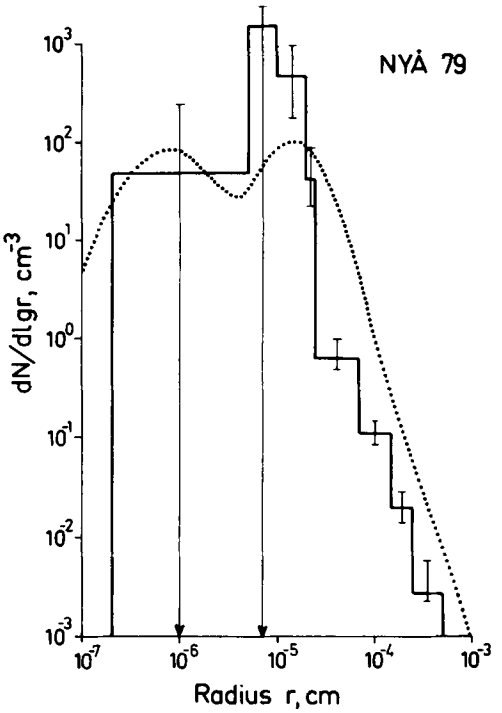

Fig. 4. Number size distribution of arctic haze inverted from integral aerosol properties measured at Ny-Ålesund, Svalbard. The global background number size distribution after Jaenicke (1979) is drawn as a dotted line.

same scattering spectrum as a smaller number of larger particles. However, the additional information for the CN-counter sets upper and lower limits for the total number of Aitken particles to be built up in the inversion. Therefore no histogram will be found with zero particles in *all* Aitken nuclei columns and the averaging over many independent solutions creates the size distribution plotted in Fig. 4. The error bars contain the variations in the inverted size distribution due to three different sources:

(a) real variations in the measured data
(b) statistical errors in the measured data
(c) ambiguities in the relationship between integral aerosol properties and differential particle size distribution.

Since there are no other data available on the size distribution of arctic haze, the Svalbard results are compared to the global background size distribution given by Jaenicke (1979) (plotted as a dotted line in Figs. 4–6). Within about one order of magnitude the Arctic haze distribution agrees with the global background. However, in the range 0.05 to 0.2μm radius there is an excess concentration of about one order of magnitude in Arctic haze. Since these particles are already small compared to visible wavelengths, they can be the cause of the remarkably bluish visual appearance of the turbid air on Spitsbergen. It should be noted that this blue haze-color was quite different from the dark "Rayleigh blue" skies observed in extremely clean air, e.g. at high altitudes. On the other hand there is a very sharp decrease in concentration with particle size from about 0.3μm radius and up to the largest sizes investigated. In this range the Arctic haze distribution remains about an order of magnitude below the global average.

The hypothesis of Arctic haze being well aged continental aerosol gives an explanation for this peculiar size distribution. The aerosol reaches the Arctic on long-distance transport paths (see for instance Rahn et al. (1979), Fig. 8). Applying the picture of particle residence times versus size given by Jaenicke (1978), this process should lead to an aerosol in the sink region (Arctic) which has peak concentrations in the 0.1 to 1.0 μm radius range. The total number of 300 particles per cm^3 agrees well with our knowledge about the large scale distribution of condensation nuclei. It can be explained by the small removal rates for Aitken nuclei when the concentration decreases to a few hundred per cm^3 (Junge, 1963).

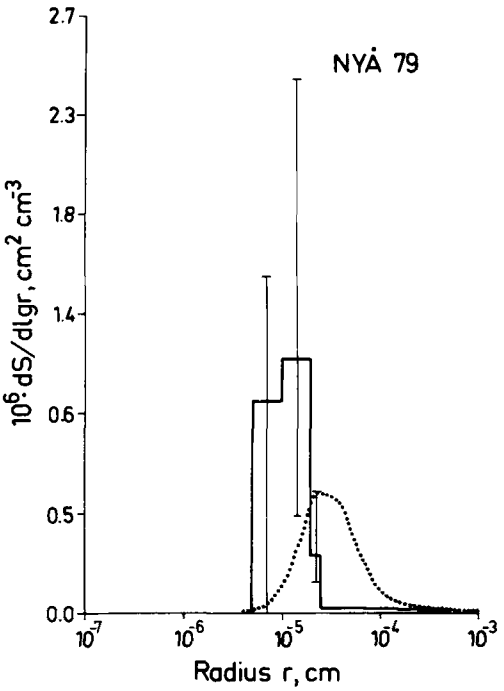

Fig. 5. Surface size distribution of Arctic haze derived from the number size distribution inverted from integral aerosol properties measured at Ny-Ålesund, Svalbard. The global background surface size distribution after Jaenicke (1979) is drawn as a dotted line.

The two higher moments of the size distribution (surface and volume) have been calculated from the inversion results. They are plotted on logarithmic/linear scales in Figs. 5 and 6. With this form of presentation the size ranges primarily contributing to integral aerosol properties like light scattering coefficients or total suspended mass can be identified directly. The comparison with the global background drawn as dotted lines in Figs. 5 and 6 is also made easier.

The peak of the surface size distribution of Arctic haze lies about one octave lower in particle size than for the global background and the grand average of the total surface is about a factor of two larger than for the global background. Taking into account the relation of scattering efficiencies versus size, the light scattering coefficients of Arctic haze particles lie on the level of the global background. However, the wavelength dependence is more

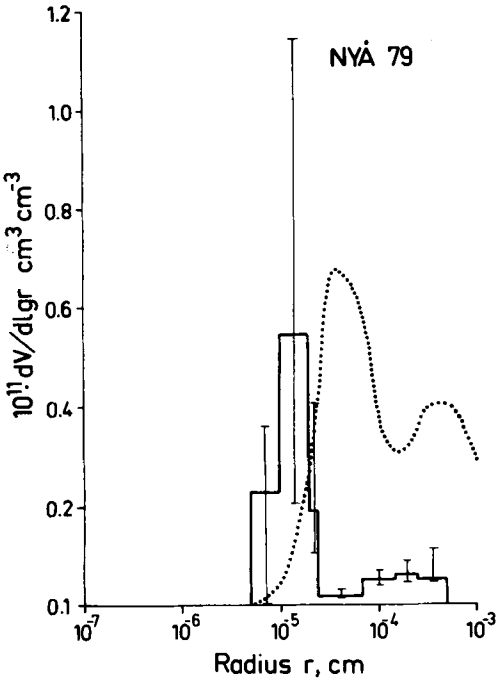

Fig. 6. Volume size distribution of Arctic haze derived from the number size distribution inverted from integral aerosol properties measured at Ny-Ålesund, Svalbard.

blue-dominated than that for the global background, model given by Jaenicke (1979).

The total suspended volume in Arctic haze is also dominated by smaller particles compared to the global background and the coarse particle mode (though not encompassed completely by the present study) is weaker in Arctic haze than in the global background, see Fig. 6. Assuming a particle density of 2 g cm^{-3} the total suspended mass at Ny-Ålesund was between 2 and 12 μg m^{-3} which compares well with the 7 μg m^{-3} for the global background. One of the reviewers verified the unusually large fraction of mass in the accumulation mode predicted by the inversion results using chemical data from Spitsbergen. Fig. 6 predicts five to six times more mass in the accumulation mode than in the coarse mode, assuming equal densities in each mode. He predicts approximately four times more mass in the accumulation mode than in the coarse mode, which is in very good agreement when all of the attendant uncertainties are considered. It becomes even better agreement when greater density is given to the coarse mode (because of the silicate particles) than to the accumulation mode.

7. Conclusions

The results of the present study at Ny-Ålesund, Svalbard, present the first consistent picture of optical properties and particle size distribution of Arctic haze. The number size distribution can be explained by a well-aged continental aerosol that has reached the Arctic sink region on long distance transport paths. Light scattering coefficients and total suspended particle volume lie on the levels of the global background. This means that the order of magnitude discrepancy between *in situ* nephelometric measurements and aerosol optical depths from solar extinction measurements in Arctic haze (Shaw, 1975), could not be resolved by the Svalbard experiment. It is clear that further Arctic studies are needed that cover both summer and winter seasons and also contain continuous solar and stellar extinction measurements in complement to the nephelometer recordings. The Swedish icebreaker expedition Ymer-80 will supply the next possibility for an extended Arctic aerosol experiment.

8. Acknowledgements

Besides the direct scientific interests, the Svalbard experiment was planned as preparation of the Arctic expedition Ymer-80 through a field test of the instruments under Arctic conditions. The support from the Ymer-80 budget is gratefully acknowledged. The stay in Ny-Ålesund would not have been possible without the generous support of the Norwegian Polar Institution and our liaison in the Norwegian scientific community, K. Henriksen, Tromsø, Norway. I gratefully acknowledge the instrument loan received from the Norwegian Institute of Air Research for the experiment. The contribution of both manpower and instruments from the Institute for Meteorology at the University of Mainz was an essential factor for the success of the experiment. B. Moberg and S. Larsson assisted in the data reduction and in the preparation of the manuscript. Finally, the constructive comments and the additional information about the mass distribution of Arctic haze by one of the reviewers are gratefully acknowledged.

REFERENCES

Charlson, R. J., Porch, W. M., Waggoner, A. P. and Ahlquist, N. C. 1974. Background aerosol light scattering characteristics: nephelometric observations of Mauna Loa Observatory compared with results at other remote locations. *Tellus 26*, 346–360.

Fenn, R. W. and Weickmann, H. K. 1959. Some results of aerosol measurements. *Geofis. pura e appl. 42*, 53–61.

Fenn, R. W. 1960. Measurements of the concentration and size distribution of particles in the Arctic air of Greenland. *J. Geophys. Res. 65*, 3371–3376.

Flyger, H., Heidam, N. Z., Hansen, K., Megaw, and Cox, L. C. 1973. The background level of the summer tropospheric aerosol over Greenland and the North Atlantic Ocean. *J. Appl. Meteor. 12*, 161–174.

Haaf, W. and Jaenicke, R. 1977. Determination of the smallest particle size detectable in condensation nucleus counters by observation of SO_2 photo-oxidation products. *J. Aerosol Sci. 8*, 447–456.

Heintzenberg, J. and Quenzel, H. 1973. Calculations on the determination of the scattering coefficient of turbid air with integrating nephelometers. *Atm. Env. 7*, 509–519.

Heintzenberg, J. 1976. Determination in situ of the size distribution of high tropospheric aerosol particles. Final Report for the G.M.C.C. programme. NOAA—Dept. of Commerce, Silver Springs, Md.

Heintzenberg, J. 1978. The angular calibration of the total scatter/backscatter nephelometer, consequences and applications. *Staub 38*, 62–63.

Heintzenberg, J., Trägårdh, C., Alm, G., Boström, R., Granat, L., Hansson, H.-Ch., Holm, B., Moritz, S., Richter, A. and Söderlund, R. 1979. Physical and chemical properties of aerosols under varying European influence. Report AC-48, Department of Meteorology, University of Stockholm.

Heintzenberg, J., Müller, H. and Quenzel, H. 1980. Aerosol size distribution inverted from optical data: The information content of extinction spectrum plus scattering function. To be submitted to *Applied Optics*.

Jaenicke, R. 1978. Über die Dynamik atmosphärischer Aitkenteilchen. Berichte Bunsenges. *Phys. Chem. 82*, 1198–1202.

Jaenicke, R. 1979. Natural aerosols. Paper presented at the Conference on Aerosols: Anthropogenic and Natural—Sources and Transport, January 1–12, New York. To be published in the *Annals of the New York Academy of Sciences*.

Junge, C. 1963. Large scale distribution of condensation nuclei in the troposphere. *J. Rech. Atm. 1*, 185–190.

Liu, B. Y. H., Berglund, R. N. and Agarwal, J. K. 1974. Experimental studies of optical particle counters. *Atm. Env. 8*, 717–732.

Mie, G. 1908. Beiträge zur Optik trüber Medien, speziell kolloidaler Metallösungen. *Ann. Phys. 4*, 377–445.

Porch, W. M., Charlson, R. J. and Radke, L. F., 1970. Atmospheric aerosols. Does a background level exist? *Science 70*, 315–317.

Rahn, K. A. 1971. Sources of trace elements in aerosols—An approach to clean air. Ph.D. Thesis, University of Michigan, Department of Atmospheric and Oceanic Sciences.

Rahn, K. A., Borys, R. D. and Shaw, G. E. 1977. The Asian source of Arctic haze bands. *Nature 268*, 713–715.

Rahn, K. A. 1978. Arctic air-sampling network. *Arctic Bulletin 2*, 343–346.

Rahn, K. A. and McCaffrey, R. J. 1979. On the origin and transport of the winter Arctic aerosol. Paper presented at the Conference on Aerosols: Anthropogenic and Natural—Sources and Transport, January 9–12, 1979, New York. To be published in the *Annals of the New York Academy of Sciences*.

Robinson, E. and Robbins, R. C. 1969. Atmospheric CO concentrations on the Greenland ice cap. *J. Geophys. Res. 74*, 1968–1973.

Scholz, J. 1932. Vereinfachter Bau eines Kernzählers. *Meteor. Z. 49*, 381–388.

Shaw, G. E. 1975. The vertical distribution of tropospheric aerosols at Barrow, Alaska. *Tellus 27*, 39–49.

Skala, G. F. 1963. A new instrument for the continuous measurement of condensation nuclei. *Anal. Chemie 35*, 702–706.

Ström, L. 1972. Transmission efficiencies of aerosol sampling lines. *Atm. Env. 6*, 133–142.

Whitby, K. T. 1978. The physical characteristics of sulfur aerosols. *Atm. Env. 12*, 135–159.

РАСПРЕДЕЛЕНИЕ ЧАСТИЦ ПО РАЗМЕРАМ И ОПТИЧЕСКИЕ СВОЙСТВА АРКТИЧЕСКОЙ ДЫМКИ

В районе Най-Алесунда, Свальбард (Исландия), проведены одновременные аэрозольные измерения с использованием счетчиков частиц и многоволнового интегрирующего нефелометра. Измеренные интегральные характеристики аэрозоля использовались для решения обратной задачи определения согласованной модели распределения по размерам частиц арктической дымки. Полученное распределение по размерам сопоставляется с глобальным распределением по размерам частиц фонового аэрозоля. Обнаружено, что как коэффициенты рассеяния света, так и общий объем взвешенных частиц соответствует уровню глобального фона.